

Generation of cylindrical vector beams in a mode-locked fiber laser using a mode-selective coupler

Yu Cai (蔡宇)¹, Jie Wang (汪杰)¹, Jiaojiao Zhang (张娇娇)¹, Hongdan Wan (万洪丹)¹,
Zuxing Zhang (张祖兴)^{1,*}, and Lin Zhang (张琳)^{1,2}

¹Advanced Photonic Technology Lab, Nanjing University of Posts and Telecommunications, Nanjing 210023, China

²Aston Institute of Photonic Technologies, Aston University, Birmingham B4 7ET, UK

*Corresponding author: zxzhang@njupt.edu.cn

Received July 17, 2017; accepted October 20, 2017; posted online November 23, 2017

We experimentally obtain cylindrical vector beams (CVBs) in a passively mode-locked fiber laser based on non-linear polarization rotation. A mode-selective coupler composed of both a single-mode fiber (SMF) and a two-mode fiber (TMF) is incorporated into the cavity to act as a mode converter from LP01 mode to LP11 mode with broad spectral bandwidth. CVBs in different mode-locked states including single-pulse, multi-pulse, and bound pulse are obtained, for the first time to our best knowledge. The ultrafast CVBs with different operation states have potential applications in many fields such as laser beam machining, nanoparticle manipulation, and so on.

OCIS codes: 060.3510, 140.3300, 140.7090.

doi: 10.3788/COL201816.010602.

Cylindrical vector beams (CVBs) have attracted considerable attention due to the axial symmetry in both polarization distribution and field amplitude^[1]. This axial symmetrical polarization leads to a range of applications, such as particle trapping^[2], high-resolution metrology^[3], material processing^[4], and electron acceleration^[5]. Over the years, a variety of methods have been developed to generate CVBs. The intracavity or extracavity involvement of the devices with axial birefringence, dichroism, or spatially variant polarization property^[6-9] to render the necessary mode discrimination against the fundamental mode forces the lasers to oscillate in CVB modes or converts spatially homogeneous polarizations into spatially inhomogeneous CVB polarizations^[10,11]. However, the use of bulky devices or a complex fabrication process seems to be a roadblock to developing compact and robust CVB fiber lasers. Generation of CVBs using few-mode fiber-based components with a function of transverse mode selection is a desirable scheme, as a few-mode step-index optical fiber can support both azimuthally polarized TE01 modes and radially polarized TM01 modes^[12,13]. By splicing two-mode fiber (TMF) to single-mode fiber (SMF) with a lateral offset and utilizing a fiber Bragg grating (FBG) written on TMF to discriminate LP01 and LP11 modes, continuous^[14-16], Q-switched^[17], and mode-locked^[18] CVB fiber lasers have been implemented. However, offset splicing inevitably induces an excess loss due to mode field mismatch, and the FBG presents a rather narrow bandwidth for mode conversion.

Mode-selective couplers (MSCs) composed of both an SMF and a few-mode fiber can convert the fundamental mode to the higher-order modes in few-mode fiber with a high conversion efficiency and broad conversion bandwidth. Mode converters based on photonic crystal fibers (PCFs)^[19] have been presented by controlling hole collapse in PCF or using the ferrule technique for joining

conventional SMFs to PCFs without splicing, with which mode conversion with a high extinction ratio has been realized. However, the used fabrication process was relatively complicated. Based on the combination of a few-mode fiber and an SMF, an MSC with a relatively simple configuration and fabrication process has been proposed by Ismael *et al.*^[20], which can excite specific higher-order modes with high efficiency and purity. Recently, femtosecond^[21] and nanosecond^[22] CVB pulse generation from mode-locked fiber lasers have been reported based on the MSC with SMF and TMF. Compared with the method of using few-mode FBG to generate CVB within a narrow bandwidth, the MSC has a lower insertion loss and can work in a broad conversion bandwidth. It is well known that a passively mode-locked fiber laser possesses diverse output states such as single pulse, multi-pulse, and bound pulse^[23-28]. Thus, it is very necessary to validate that it is still possible to generate CVB pulses in different operation regimes. Moreover, CVB pulses under different operation states may have different potential applications under different fields of particle trapping and material processing.

In this Letter, we have demonstrated nonlinear polarization rotation based mode-locked CVB fiber laser with MSC for transverse mode selecting. As a result, radially and azimuthally polarized beams in different mode-locked states have been obtained from the passively mode-locked fiber laser.

The schematic of the MSC to generate the LP11 mode is shown in Fig. 1. The working principle of the MSC is a coupled-mode mechanism of appeasing the phase-match condition in the fused fibers. To maintain the geometry of the two fibers and ensure accurate modal conversion efficiency, the MSC was fabricated using the weak fusion technique. In order to meet phase-match conditions between the LP01 mode in the SMF and the mode in

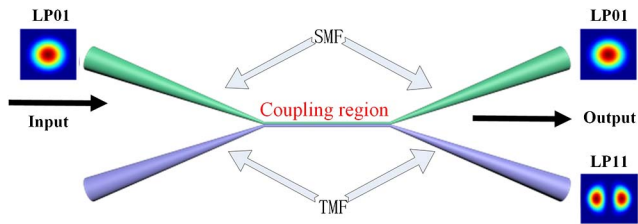


Fig. 1. Schematic of MSC.

the TMF, the SMF was pre-tapered to about $79\ \mu\text{m}$ according to the simulations^[22]. Then the pre-tapered SMF was carefully aligned with the TMF, and fused together using the modified flame brushing technique. With the tunable laser source launched into the SMF input, the powers of both the SMF and TMF output ports were monitored simultaneously by power meter. The mode field distributions at the TMF output port at different wavelengths were also detected by a CCD camera (CinCam IR), as shown in Fig. 2. The fabricated MSC can convert the LP01 mode efficiently to the LP11 mode with a low insertion loss of about 0.65 dB. Measured by the tight bend approach, the maximal purity of the converted LP11 mode can reach 97% at a wavelength of 1550 nm. It should be noted that four-mode or multi-mode fibers also support CVB modes, so they can replace the TMF for the MSC fabrication.

The experimental setup of the proposed mode-locked fiber laser based on nonlinear polarization rotation with CVB generation is shown in Fig. 3. The gain medium is heavily doped erbium-doped fiber (EDF) with a length of 1.1 m, which is pumped by two 980 nm laser diodes with the maximum pump power of 700 mW through a 980/1550 nm wavelength division multiplexing coupler (WDM) for backward pumping and a Tap + Isolator + WDM hybrid device for forward pumping. The EDF has a group velocity dispersion (GVD) of $79.4\ \text{fs}^2/\text{mm}$ at 1550 nm. A polarization-dependent isolator (PDI) is placed between two polarization controllers (PCs) as a mode-locking element to play double roles of isolating

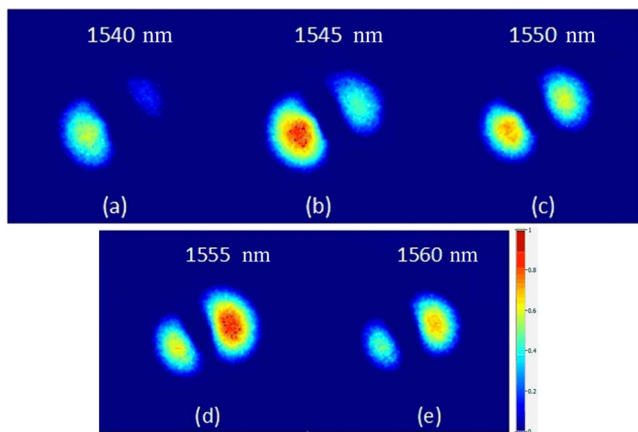


Fig. 2. CCD images of the LP11 mode excited in the TMF at different launching wavelengths.

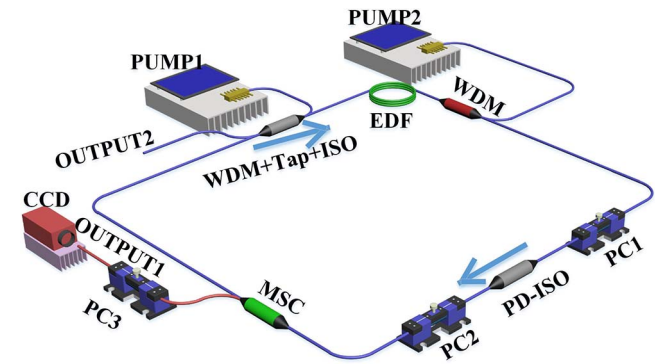


Fig. 3. Experimental setup of the proposed mode-locked fiber laser based on nonlinear polarization rotation with CVB generation.

and polarizing. The MSC is located at the laser cavity behind the second PC. The total cavity length is about 5.5 m and the net dispersion is calculated to be about $-0.013\ \text{ps}^2$.

The laser has two output ports: Output1 is the TMFs port of the MSC that is added to the mode-locked fiber laser cavity to get CVBs, and Output2 comes from the 10% tap output from the Tap + Isolator + WDM hybrid device. Output2 is used to extract the signal within the cavity to monitor the working state. The mode-locking mechanism is based on nonlinear polarization rotation effect. The basic principle of nonlinear polarization-rotation-based mode-locking is intensity-dependent saturable absorption, i.e., the lower-intensity part being absorbed and the higher-intensity part passing. The output spectrum of Output2 was measured using an optical spectral analyzer with a resolution of 0.02 nm (YOKOGAWA AQ6370D). At the same time, the time-domain waveform of Output2 was measured with an oscilloscope (SDA 6000A) with a photodetector (PD). The output beam profiles from Output1 were recorded by a CCD camera. PC3 is located on Output1 and, through adjusting the pressure and rotating PC3, the MSC can output radially and azimuthally polarized beams, respectively. It should be noted that PC3 is mounted outside the laser cavity and obviously has no influence on the light in the laser cavity.

When the pump power is above the threshold value of mode locking, mode-locked pulses can routinely be attained. Moreover, depending on the pump power and the polarizations, various output states: single pulse, multi-pulse, and bound pulse have been observed, as a common mode-locked fiber laser. Figure 4(a) shows the typical output spectrum of the mode-locked pulse from Output2, when the powers of the two pump lasers are both 450 mW. The central wavelength is located at 1560 nm, and the 3 dB bandwidth is measured to be 57.5 nm. The corresponding pulse train is shown in Fig. 4(b). The pulse repetition rate is 36.08 MHz, which is just the fundamental frequency. For single pulse operation, a commercial frequency-resolved optical gating (FROG) is used to

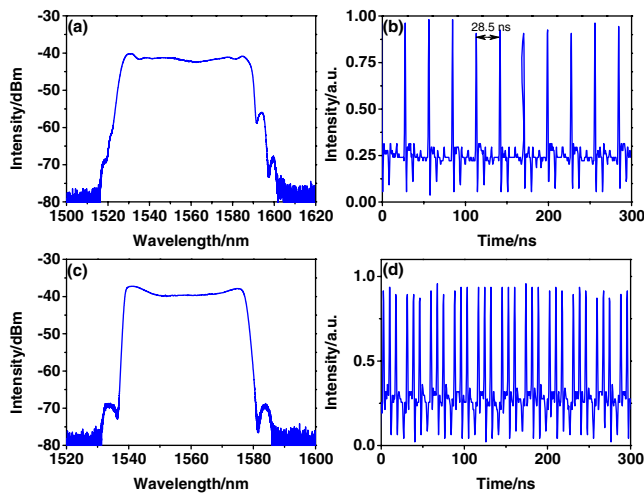


Fig. 4. (a) Spectrum and (b) the corresponding pulse train of single-pulse mode locking, (c) the spectrum and (d) the corresponding pulse train of three-pulse mode locking.

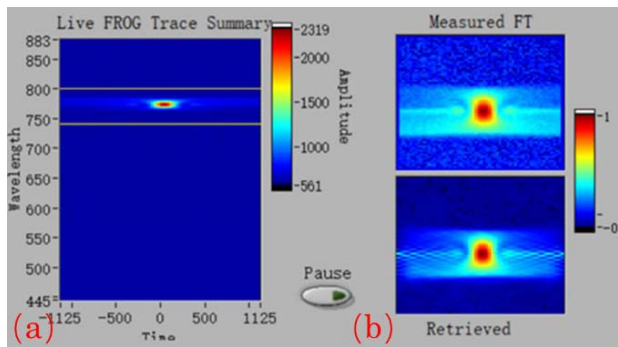


Fig. 5. (a) Live FROG trace. (b) Measured and retrieved FROG traces.

measure the pulse duration. The measured and retrieved FROG traces of the signal from Output2 are shown in Fig. 5. The autocorrelation trace is illustrated in Fig. 6. The result shows that the pulse duration is measured to be 175 fs. It is larger than the value 62 fs of the

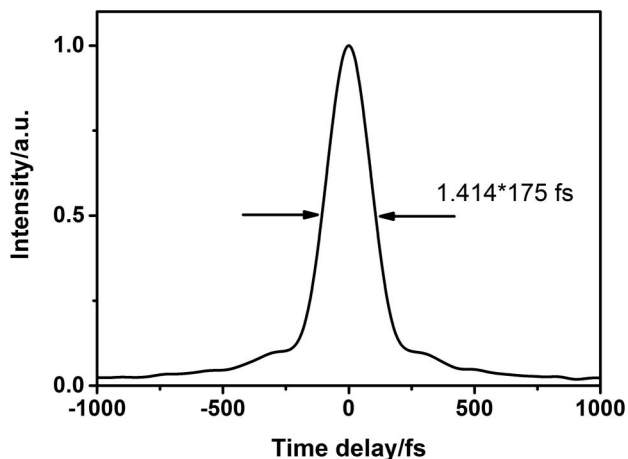


Fig. 6. Autocorrelation trace.

transformation limited pulse, which we believe can be attained through further optimizing the fiber length between the output coupler and the FROG.

In the case of keeping the pump power unchanged by adjusting the PC1 and PC2, the optical spectrum with a narrower bandwidth due to multi-pulse formation can be observed. This is to say that the laser operates in a multi-pulse state with an integer number of pulses co-existing in the cavity. By tuning PC1 and PC2, when the number of pulses in the experiment is 3, the spectrum of the multi-pulse state is the most flat, as shown in Fig. 4(c), and there is almost no continuous wave component. The 3 dB spectral bandwidth is only 35.75 nm. From the three-pulse mode-locking pulse train in Fig. 4(d), it is evident that 3 pulses per period can be distinguished. The mechanism of the multi-pulse generation^[29] is that the energy of the dissipative soliton pulse in the passive mode-locked fiber laser should be determined by the parameters of the laser cavity. Since the dissipative soliton pulse is periodically disturbed in the fiber laser cavity, the excess energy has to be radiated in the form of dispersive waves. Thus, some dispersive waves coherently superimpose to form a new pulse.

By continuing to adjust PC1 and PC2, the mode-locked CVB fiber laser reported in this Letter can output the bound pulse state. The multiple dissipative solitons in the laser have an interaction when they overlap slightly. A direct interaction between neighboring dissipative solitons leads to the generation of stable bound solitons with a fixed pulse interval and fixed phase difference that is characterized by highly contrasted fringes in its spectrum. The typical spectrum of the bound mode-locking state is shown in Fig. 7, exhibiting an interfringe interval of 0.58 nm. In the 3 dB bandwidth range, the spectrum is divided into 64 wavelengths. The corresponding pulse train is still showing a repetition rate of 36.08 MHz, as in Fig. 8, since the temporal separation of two pulses inversely proportional to the interfringe interval in the

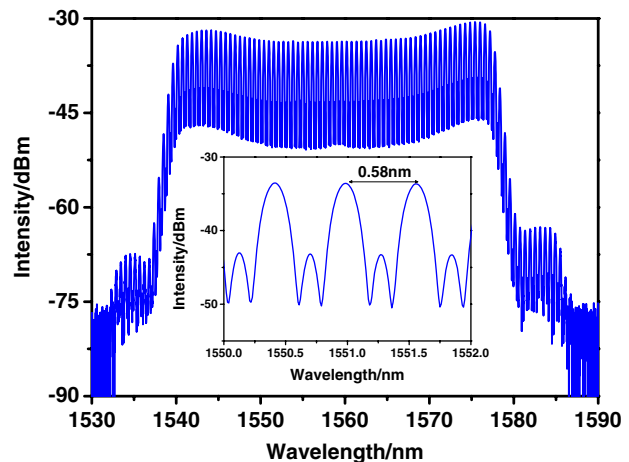


Fig. 7. Spectrum of bound mode-locking state (the inset is the close-up spectrum from 1550 to 1552 nm).

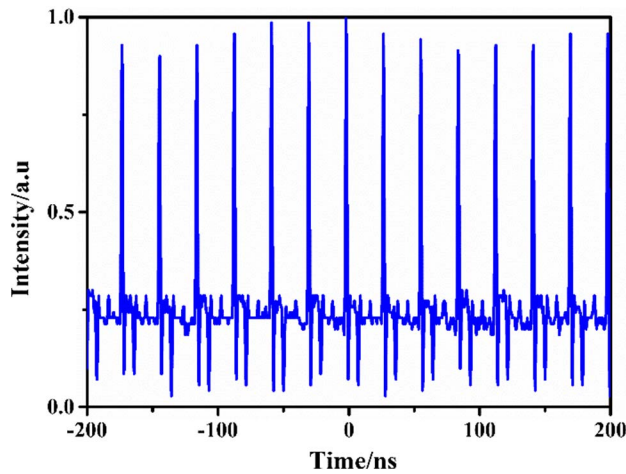


Fig. 8. Pulse train of bound mode-locking state.

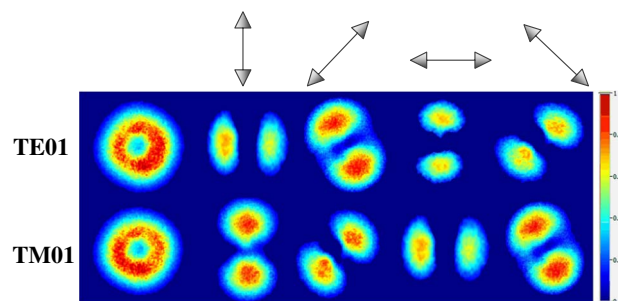


Fig. 9. Intensity distributions of (a) TE01 and (f) TM01 modes, and their evolutions with rotation of the linear polarizer.

spectrum in the picosecond range cannot be resolved by the oscilloscope.

In order to verify the CVB generation under the different states of the mode-locked fiber laser reported in this Letter, intensity distributions from Output1 have been simultaneously recorded with a CCD camera. The doughnut-shaped intensity profiles of the radially and azimuthally polarized beams have always been observed, as shown in Figs. 9(a) and 9(f). To further demonstrate the polarization distribution of the output beam, the polarizer was inserted into the path between the TMF output and the CCD camera. The TE01 or TM01 mode can be discriminated through carefully adjusting PC3, based on the principle of extrusion and torsion^[30]. The results with the white arrow indicating the orientation of the linear polarizer are shown in Figs. 9(b)–9(e) and 9(g)–9(j), respectively. As shown in Figs. 9(b)–9(e), the direction of the passed light rotates with the orientation of the polarizer, and is always perpendicular to the orientation of the polarizer, thus the output laser beam is azimuthally polarized. Contrarily, the direction of the passed light is always parallel to the orientation of the polarizer in Figs. 9(g)–9(j), and the output laser beam is radially polarized accordingly.

In conclusion, we demonstrate a mode-locked CVB fiber laser with different mode-locked states based on the MSC.

This proves that CVBs can be obtained not only in a traditional single pulse state, but also in various mode-locked states of multi-pulses and bound pulses. The ultrafast CVBs with different operation states with unique characteristics in temporal and spatial domains may have potential applications in many fields such as laser beam machining, nanoparticle manipulation, and so on.

This work was supported by the National Science Foundation of Jiangsu Province (Nos. BK20161521 and BK20150858), the Nanjing University of Posts and Telecommunications (NUPTSF) (Nos. NY214059, NY214002, and NY215002), the Distinguished Professor Project of Jiangsu (No. RK002STP14001), the Six Talent Peaks Project in Jiangsu Province (No. 2015-XCL-023), and the Postgraduate Research & Practice Innovation Program of Jiangsu Province (Nos. SJCX17_0234 and KYCX17_0744).

References

1. Q. Zhan, *Adv. Opt. Photon.* **1**, 1 (2009).
2. H. Kawauchi, K. Yonezawa, Y. Kozawa, and S. Sato, *Opt. Lett.* **32**, 1839 (2007).
3. L. Novotny, M. R. Beversluis, K. S. Youngworth, and T. G. Brown, *Phys. Rev. Lett.* **86**, 5251 (2001).
4. M. Meier, V. Romano, and T. Feurer, *Appl. Phys. A* **86**, 329 (2007).
5. D. N. Gupta, N. Kant, E. K. Dong, and H. Suk, *Phys. Lett. A* **368**, 402 (2007).
6. K. Yonezawa, Y. Kozawa, and S. Sato, *Opt. Lett.* **31**, 2151 (2006).
7. X. L. Wang, J. Ding, W. J. Ni, C. S. Guo, and H. T. Wang, *Opt. Lett.* **32**, 3549 (2007).
8. Q. Zhan and J. R. Leger, *Appl. Opt.* **41**, 4630 (2002).
9. D. Lin, K. Xia, J. Li, R. Li, K. Ueda, G. Li, and X. Li, *Opt. Lett.* **35**, 2290 (2010).
10. Y. Kozawa and S. Sato, *Opt. Lett.* **30**, 3063 (2005).
11. C. Maurer, A. Jesacher, S. Fürhapter, S. Bernet, and M. Ritsch-Marte, *New J. Phys.* **9**, 78 (2007).
12. G. Volpe and D. Petrov, *Opt. Commun.* **237**, 89 (2004).
13. S. Ramachandran, P. Kristensen, and M. F. Yan, *Opt. Lett.* **34**, 2525 (2009).
14. B. Sun, A. Wang, L. Xu, C. Gu, Z. Lin, H. Ming, and Q. Zhan, *Opt. Lett.* **37**, 464 (2012).
15. W. Zhang, L. Huang, K. Wei, P. Li, B. Jiang, D. Mao, F. Gao, T. Mei, G. Zhang, and J. Zhao, *Opt. Express* **24**, 10376 (2016).
16. H. Wan, H. Li, C. Wang, B. Sun, Z. Zhang, W. Wei, and L. Zhang, *IEEE Photon. J.* **9**, 7100608 (2017).
17. J. Lin, K. Yan, Y. Zhou, L. Xu, C. Gu, and Q. Zhan, *Appl. Phys. Lett.* **107**, 197 (2015).
18. B. Sun, A. Wang, C. Gu, G. Chen, L. Xu, D. Chung, and Q. Zhan, *Opt. Lett.* **40**, 1691 (2015).
19. A. Witkowska, S. G. Leon-Saval, A. Pham, and T. A. Birks, *Opt. Lett.* **33**, 306 (2008).
20. R. Ismael, T. Lee, B. Oduro, Y. Jung, and G. Brambilla, *Opt. Express* **22**, 11610 (2014).
21. T. Wang, F. Wang, F. Shi, F. Pang, S. Huang, T. Wang, and X. Zeng, *J. Lightwave Technol.* **11**, 2161 (2016).
22. H. Wan, J. Wang, Z. Zhang, Y. Cai, B. Sun, and L. Zhang, *Opt. Express* **25**, 11444 (2017).
23. D. Y. Tang, L. M. Zhao, and B. Zhao, *Appl. Phys. B* **80**, 239 (2005).
24. X. Liu, *Phys. Rev. A* **81**, 023811 (2010).

25. J. Peng, L. Zhan, S. Luo, and Q. Shen, *IEEE Photon. Technol. Lett.* **25**, 948 (2013).
26. Z. Wang, S. Du, J. Wang, F. Zou, Z. Wang, W. Wu, and J. Zhou, *Chin. Opt. Lett.* **14**, 041401 (2017).
27. Z. Wang, Z. Wang, Y. Liu, R. He, G. Wang, G. Yang, and S. Han, *Chin. Opt. Lett.* **15**, 080605 (2017).
28. F. Zhao, Y. Wang, Y. Wang, H. Wang, and Y. Cai, *Chin. Opt. Lett.* **15**, 101402 (2017).
29. Y. Lyu, X. Zou, H. Shi, C. Liu, C. Wei, J. Li, H. Li, and Y. Liu, *Opt. Express* **25**, 13286 (2017).
30. S. Li, Q. Mo, X. Hu, C. Du, and J. Wang, *Opt. Lett.* **40**, 4376 (2015).